Saudi Journal of Biological Sciences (2019) **26**, 8–19

King Saud University

Saudi Journal of Biological Sciences

www.ksu.edu.sa
www.sciencedirect.com

ORIGINAL ARTICLE

Transcriptional analysis of tyrosinase gene expression during *Bufo bufo* development

Patrizia Cesare, Antonella Bonfigli, Michele Miranda *, Anna Maria Poma, Sabrina Colafarina, Osvaldo Zarivi

Department of Life, Health and Environmental Sciences, University of L'Aquila, 67100 L'Aquila, Italy

Received 2 March 2016; revised 8 September 2016; accepted 24 October 2016
Available online 2 November 2016

KEYWORDS

Amphibian egg;
Tyrosinase;
Pigment cell;
Melanin;
Oxygen

Abstract Tyrosinase (EC.1.14.18.1.) is a widespread enzyme, in the phylogenetic scale, that produces melanin, from bacteria to man, by using as substrates monophenols, o-diphenols and molecular oxygen. In this work we have confirmed and demonstrated that during *Bufo bufo* development tyrosinase activity and gene expression first occur at developmental stages 17–18 (tail bud-muscular response) as detected by a spectrophotometric assay and qRT-PCR. As expected, also during *B. bufo* development tyrosinase gene is expressed after the late gastrula (stage 12), differently from *Rana pipiens* development when tyrosinase mRNA appears at the neural plate stage and enzyme activity at stage 20 (gill circulation). We have cloned and sequenced the *B. bufo* tyrosinase cDNA in order to prepare *B. bufo* tyrosinase cDNA specific primers (forward and reverse). Tyrosinase mRNA cloning has been performed by using degenerate primers prepared according to the anuran tyrosinase gene sequence coding for the copper binding sites. The expressions of tyrosinase gene and enzymatic activity during *B. bufo* development support that until the developmental stage 17, embryo melanin is of maternal origin and at this stage can start embryo melanin synthesis. A correlation exists between tyrosinase expression and O_2 consumption during *B. bufo* development.

1. Introduction

The animal pole of the amphibian egg is heavily pigmented; the pigment is eumelanin (Taylor and Hadley, 1972; Eppig and Dumont, 1974) and is synthesized by the enzyme tyrosinase (EC 1.14.18.1; monophenol, dihydroxyphenylalanine: oxygen oxidoreductase) from L-tyrosine (Mason, 1965; Nicolaus, 1968; Robb, 1984; Prota, 1992; Sanchez-Ferrer et al., 1995). The occurence of melanin at the animal pole of the amphibian egg, where the cell nucleus is located, may be related to photoprotection (Bagnara, 1985; Prota, 1992). The amphibian egg has been also considered as a pigment cell (Bagnara, 1985); the occurrence of melanin at the animal pole has been also related, to the warming of the egg and embryo by absorption of solar radiation (Bagnara, 1985; Solano, 2014).

We have previously investigated the expression of tyrosinase activity during *Bufo bufo* development, by using biochem-

* Corresponding author. Fax: +39 862 433273.
E-mail address: michele.miranda@univaq.it (M. Miranda).
Peer review under responsibility of King Saud University.

Production and hosting by Elsevier

http://dx.doi.org/10.1016/j.sjbs.2016.10.018
1319-562X

ical techniques (Miranda et al., 1982). A very feeble tyrosinase activity has been found by polyacrylamide disc gel electrophoresis during development, from the first cleavage till muscular response stages, but none by spectrophotometer in the extracts of melanosomes until developmental stage 19 (Miranda et al., 1982). During *Rana pipiens* development the tyrosinase enzymatic activity gradually increase from the neural plate stage till stage 19 (heart beat) (Benson and Triplett, 1974; Gaulton and Triplett, 1983).

The aim of this work is to detect when during *Bufo bufo* development the embryo tyrosinase gene is transcriptionally expressed and thus eumelanin other than that of maternal origin, can be produced. In order to address this question we prepared *B. bufo* tyrosinase specific primers to detect by Real-time quantitative PCR (qRT-PCR) the expression of tyrosinase mRNA during *B. bufo* development. It is of some interest to investigate if tyrosinase, an oxygen using enzyme, is expressed when oxygen is transported to the tissues. During amphibian development cytochrome oxidase and respiration highly increases from the tail bud stage (Boell et al., 1971; Hastings and Burggren, 1995); thus we have also investigated if some relationship exists between tyrosinase activity and oxygen consumption during *B. bufo* development (Petrucci, 1961).

2. Materials and methods

2.1. Bufo bufo embryo collection

The eggs of *B. bufo* were collected along the banks of the lake Pietranzoni 900 m s.l.m. near L'Aquila Abruzzo (Italy). The eggs were kept at 12–14 °C in tap water. Jelly was removed from early embryonic stages by treatment with 0.5% sodium thioglycolate at pH 8.6 in a ratio of 1:1 (v/v). The embryos were staged by reference to Shumway (1940). At the selected developmental stages (stage 7, sixth cleavage; stage 12, late gastrula; stage 17, tail bud; stage 18, muscular response; stage 20, gill circulation; stage 22, tail fin circulation; stage 25, operculum complete) 160 embryos at different development stages were used to isolate and purify melanosomes in order to measure tyrosinase activity; 50 embryos at the different developmental stages were used for RNA purification.

2.2. Melanosome preparation

Melanosomes were purified from *B. bufo* embryo homogenates at various stages of development, at 12–14 °C. Homogenates (2 ml), diluted with 0.10 M potassium phosphate buffer, pH 7.0, in a 1:1 (v:v) ratio, were layered on a discontinuous sucrose density gradient (1.8 M sucrose, 2 ml, and 1.4 M sucrose, 1 ml) and centrifuged for 60 min at 100,000*g*. The pellets were resuspended in 2 ml of the same buffer and centrifuged as above. The final pellets consisted mainly of melanosomes. Protein concentration was determined by the biuret method, using bovine serum albumin as a standard.

2.3. Tyrosinase assay and polyacrylamide gel electrophoresis

Tyrosinase activity was spectrophotometrically measured by using the dopachrome assay procedure with L-3,4-dihydroxyphenylalanine (L-DOPA) as substrate. 5 mM L-DOPA in sodium phosphate buffer (0.1 M pH 6.8) and melanosome extract, in a total volume of 1.0 ml were incubated at 25 °C; the dopachrome formation was monitored continuously by measuring the absorbance increase at 475 nm (Mason, 1948).

To determine the active form of tyrosinase, 15 μg of protein from the melanosome extract was loaded onto 8% (w/v) polyacrylamide gel (Laemmli, 1970). Running buffer and gels contained 0.1% sodium dodecyl sulfate (SDS), but the samples were not heated and mercaptoethanol was omitted from the loading buffer. After electrophoresis, the gels were stained for catecholase activity with 5.0 mM L-DOPA in 0.1 M phosphate buffer pH 6.8 for 120 min. Electrophoresis was performed at 4 °C, at a constant current of 25 mA. Controls with a tyrosinase inhibitor, 1.0×10^{-4} M phenylthiourea (PTU), were done. The protein bands were shown by 0.1% Coomassie brilliant G250 blue staining.

2.4. Determination of melanin content

50 *B. bufo* embryos at different development stages were suspended in 0,1 mM sodium phosphate buffer, pH 6.8, at 1:5 ratio (w/v) and were sonicated 5 times on ice (20 s/8 cycles/50% power), with Bandelin, Sonopuls D2070 sonicator (Berlin, Germany). Then, Brij 35 was added to the suspension at a final concentration of 0.1%; samples were homogenized with a Potter–Elvehjem homogenizer, motor driven for 10 cycles of 2 min at intervals of 15 s, and protein content was determined. Melanin content was determined as reported (Seyeon et al., 2013) with minor modifications. NaOH (4 N), containing 10% dimethyl sulfoxide, was added to the samples in the ratio 1:1, and these were homogenized for 10 cycles of 2 min at intervals of 30 s. The samples were incubated at 70 °C for 120 min, shaken vigorously every 10 min and centrifuged for 5 min at 10,000*g*. The melanin content of the supernatant was spectrophotometrically determined as the absorbance at 405 nm. The obtained values were normalized to the total protein concentration.

2.5. RNA extraction, purification and cDNA synthesis

Total RNA was isolated from different embryonic stages (50 pooled individuals). RNase-free mortars and pestles were used in combination with liquid nitrogen to disrupt frozen tissue samples into a powder with the RNAqueous™ (Ambion Huntingdon, Cambridgeshire, UK) kit as described by the manufacturer and treated with DNAse (Roche Diagnostic GmbH, Penzberg, Germany). Then, the RNA was treated with Recombinant RNase-free DNAse I from bovine pancreas (Roche Diagnostics, Indianapolis, USA) according to the manufacturer's instructions. The purity of all RNA samples was assessed at absorbance ratios of A260/A280 and A260/A230 using a Nanodrop 2000 spectrophotometer (Thermo Scientific, Waltham, WA) and the integrity of the RNA was immediately checked using 1.2% agarose gel electrophoresis (1.3 μg samples). RNA concentration was calculated based on absorbance values at 260 nm, and RNA samples were stored at −80 °C until use. RNA was used as a template for reverse transcriptase (RT); cDNA was generated from 1 μg of total RNA by Superscript III First-Strand Synthesis SuperMix for qRT-PCR (Invitrogen by Life Technologies, Carlsbad, CA, USA), according to the manufacturer's instruction. The

2 × RT Reaction Mix includes oligo(dT)20, random hexamers, $MgCl_2$, and deoxynucleotides (dNTPs) in a buffer formulation that has been optimized for qRT-PCR. *Escherichia coli* RNase H was used in the kit to remove the RNA template from the cDNA:RNA hybrid molecules after first-strand synthesis. Absence of DNA was checked by comparing cDNA samples with RNA samples which were not reverse transcribed (minus RT control). The obtained cDNAs were used for polymerase chain reaction (PCR) and qRT-PCR.

2.6. PCR, cloning and sequencing

Partially degenerate PCR primers (FORREVBB) were designed from conserved regions of tyrosinase genes: *Rana nigromaculata* (GenBank accession number D12514), *Xenopus laevis* (GenBank accession number BC043815), *Rana galamensis* (GenBank accession number AY341749.1), *Bufo japonicus* (GenBank accession number AB612059) *Leptodactylus fuscus* (GenBank accession number AY341760.1), *Rana temporaria* (GenBank accession number AF249182.1). PCR was performed using 1 μL of cDNA as template (500 ng). PCR conditions were: 10 ×buffer (New England Biolabs), 0.6 mM dNTPs, 0.4 mM primers (each) and 1.25 U Taq DNA polymerase (New England Biolabs) in a 50 μL reaction mix. After amplification, fragments of the expected size were gel-extracted using S.N.A.P. UV-Free Gel Purification Kit (Invitrogen-Life science) and cloned using the TOPO TA kit (Invitrogen-life technologies) according to the manufacturers' directions. The found active site sequence coding for tyrosinase were used for the synthesis of the specific primers (BFGSP1, BFGSP2, BRGSP1, BRGSP2) as shown in Table 1. The specific primers were used with the kit "3′ RACE and 5′ RACE System for Rapid Amplification of cDNA Ends", in accordance with the instructions (Invitrogen-life technologies). Then the specific primers (EXPRFOR, EXPRREV), shown in Table 1, were used to detect *B. bufo* tyrosinase mRNA expression at the different developmental stages. The amplification products were resolved by 1.5% agarose gel electrophoresis in Tris acetate-EDTA (TAE) buffer (running conditions: 90 V for 90 min) and stained with ethidium bromide. Band sizes were checked by using the Invitrogen Trackit 100 bp DNA ladder.

2.7. Quantitative Real-Time PCR

In this study, after a detailed search in the literature, three housekeeping genes were selected (16S rRNA, Histone H4, NADH dehydrogenase subunit I), these genes are among the most common ones frequently used, as reference genes, for normalization of qRT-PCR. Two couples of primers were prepared on the base of *B. bufo* tyrosinase sequence. To facilitate the qRT-PCR analysis of all the investigated genes under the same reaction conditions, primers were designed using Primer Express 3.0 software (PE Applied Biosystems, USA) under default parameters. The PCR primer sequences used to quantitate the expression of all the genes are shown in Table 1. All the RNA samples were tested for genomic DNA contamination by qRT-PCR negative controls of cDNA samples omitting reverse transcriptase. In all of the negative control samples no amplification of the fluorescent signal was detected, thus proving that the extraction procedure, including the DNAse treatment, effectively removed genomic DNA from all of the RNA samples.

As an exogenous control, 106 copies of pAW101 RNA (GeneAmp Gold RNA PCR Control Kit by Life Technologies Carlsbad, CA, USA)/μg of RNA extracted were added to each sample. The two control primers (DM151, DM152) included in this kit amplified a 308 bp product. Real-time PCR was performed using an Applied Biosystems 7300 Real-Time PCR System and software (Applied Biosystems, Foster City, USA). qRT-PCR was performed with the SYBR GreenER™ qPCR SuperMix for ABI PRISM, which is a ready-to-use cocktail containing all components (including ROX Reference Dye at a final concentration of 500 nM), except primers and template. The PCR Mastermix contained the primers (1 μL primer pair mix of 10 μM primer pair stock), 25 μL of 2*x* GreenER™ qPCR SuperMix for ABI PRISM (Applied Biosystems), 1 μL of diluted cDNA (corresponding to 1 ng) and sterile nuclease free water to a final volume of 50 μL. All the PCRs were performed under following conditions: 2 min at 50 °C, 10 min at 95 °C, and 40 cycles of 15 s at 95 °C and 60 s annealing and extension at 60 °C in 96-well optical reaction plates (Applied Biosystems, USA). The specificity of the qRT-PCR reactions was monitored by the melting curve analysis (60–95 °C), after 40 cycles, using SDS software (version 1.4, Applied Biosystems) shown in Fig. 1. Three biological replicates for each sample were used for Real-time PCR analysis and three technical replicates were analyzed for each biological replicate; a single peak was observed and this confirms the synthesis of a single product.

2.8. Standard curve construction and Real-time PCR

To ensure the reliability of the amplification results, the qRT-PCR amplification efficiencies were determined by the standard curve and melting curve analyses. Standard curves were constructed by using serially diluted cDNA as a template prior to the candidate gene expression analysis. Each template used in the qRT-PCR amplification was analyzed by three independent runs. PCR efficiencies and regression coefficients were calculated by the QGene software (Version 4.3.10). For all the primers, a single peak was observed, thus confirming the synthesis of a single product that was further validated, as shown in Fig. 1, by analysis of the qRT-PCR product on a 2.5% agarose gel. Gene expression analyses were conducted by an Applied Biosystems 7300 Real-Time PCR System using the SYBR GREEN method as indicated above.

2.9. Expression stability analysis of candidate reference genes

We used the RefFinder tool (http://fulxie.0fees.us/?type=reference) for the assessment and screening of the reference genes (16S rRNA, Histone H4, NADH dehydrogenase subunit I). The RefFinder tool integrates the currently available major computational programs (geNorm, Normfinder, BestKeeper and the Comparative CT method, (Pfaffl et al., 2004; Andersen et al., 2004; Vandesompele et al., 2002; Silver et al., 2006) to compare and rank the tested candidate reference genes (data not shown).

Table 1 Primers used in this study. Primer sequences, accession numbers, amplicon sizes and PCR efficiencies are indicated.

Gene name	Accession number	Primer name	Primer sequence 5′–3′; Tm (°C).	Product (bp)	(%)PCR efficiency
Primer sequences used to clone and amplify tyrosinase mRNA *Bufo bufo*					
Degenerate PCR primers conserved regions of tyrosinase genes CuA	D12514; BC043815; AY341749.1; AB612059; AY341760.1; AF249182.1	FORREVBB	F: 5′-GGNAACTTYATGGGNTAYAAYTG-3′ R: 5′-TGCAGCCANACRAASAGRTCRTA-3′	268	
Regions of tyrosinase genes CuA	FM864217.1	BFGSP1	F: 5′-CAAGTTCATCGCCTACCTCAAT-3′ (60.1)		
		BFGSP2	F: 5′-AAACGCACCATsCAGCCCAGAC-3′ (62.4)		
		BRGSP1	R: 5′-GTCTGGGCTGATGGTGCGTTT-3′ (62.6)		
		BRGSP2	R: 5′-ATTGAGGTAGGCGATGAACTTG-3′ (60.0)		
Tyrosinase	FM864217.1	EXPR	F: 5′-CACCATGAGAGGTAGTATCATGATA-3′ (62.9) R: 5′-TCATAGATTGGACTGGTAAGTGCT-3′ (62.6)	1510	
NADH dehydrogenase subunit I	JQ348484.1	EXNADH	F:5′ GCCTCAAATTCCAAGTACGC 3′ (59.7) R: 5′ GGTGGAGGATCCCAAGAAAA 3′ (59.8)	378	
qRT-PCR assay sequences of primers					
16S rRNA	AY555020.1	BB16S	F: 5′-CCAATACACTTGAACAACGAACCA-3′ (59.3) R: 5′-GAGACCCTGATCCAACATCGA-3′ (59.8)	110	98.44
Histone H4	AY675291.1	BOFORH4	F: 5′-GCATCACCAAGCCTGCCAT-3′ (58.8) R: 5′-GAAGACTTTCAGCACCCCG-3′ (58.8)	101	98.87
NADH dehydrogenase subunit I	JQ348484.1	BOFORNADH	F: 5′-AGCCCTCTCAAGCCTCACTGT-3′ (61.8) R: 5′-CGTATGAAATCGTCTGCGCTACT-3′(60.6)	109	96.79
Tyrosinase	FM864217.1	TYR1	F: 5′-CCATGGACCGCAATGCTAAC-3′ (59.4) R: 5′-GTGCAGGGAATTGTGCATGT-3′ (57.3)	110	98.74
Tyrosinase	FM864217.1	*TYR2*	F: 5′-GCCACTGGGACCTACGAACA-3′ (61.4) R: 5′-CGCATCCCTGGAGGAGTAATAG-3′ (62.1)	108	99.29
IL1-alpha	pAW109 control RNA (Applied Biosystems_)	DM151	F: 5′–GTCTCTGAATCAGAAATCCTTCTATC-3′ (54.9) R: 5′-CATGTCAAATTTCACTGCTTCATCC-3′ (57.2)	308	98.70

Accession numbers are given for each gene used in this study: GenBank, NCBI (National Center for Biotechnology). Sequences of qRT-PCR primers were designed using the Primer Express®Software version 3.0 (Applied Biosystems), F and R refer to forward and reverse primers, respectively.

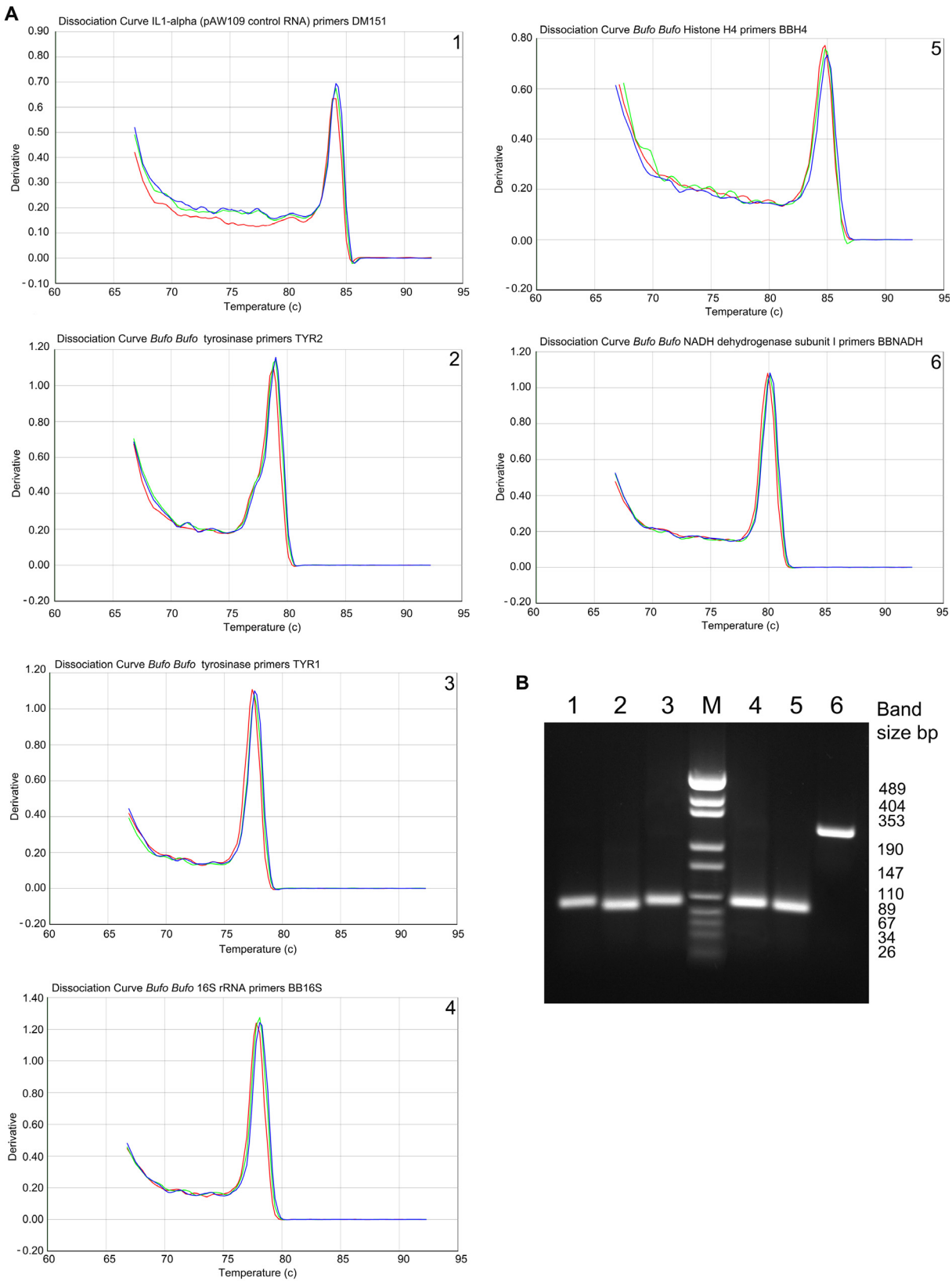

Figure 1 Specificity of qRT-PCR amplification. (A) Melting curves of the 3 reference genes, tyrosinase and (6) pAW109 control SYBR-Green qRT-PCR shows a single peak. (B) Agarose gel (2.5%) electrophoresis showing amplification of a specific qRT-PCR product of the expected size, (1) 16S rRNA, (2) histone H4, (3) NADH dehydrogenase subunit I, (4) tyrosinase 1, (5) tyrosinase 2 and pAW109 control. DNA ladder (M).

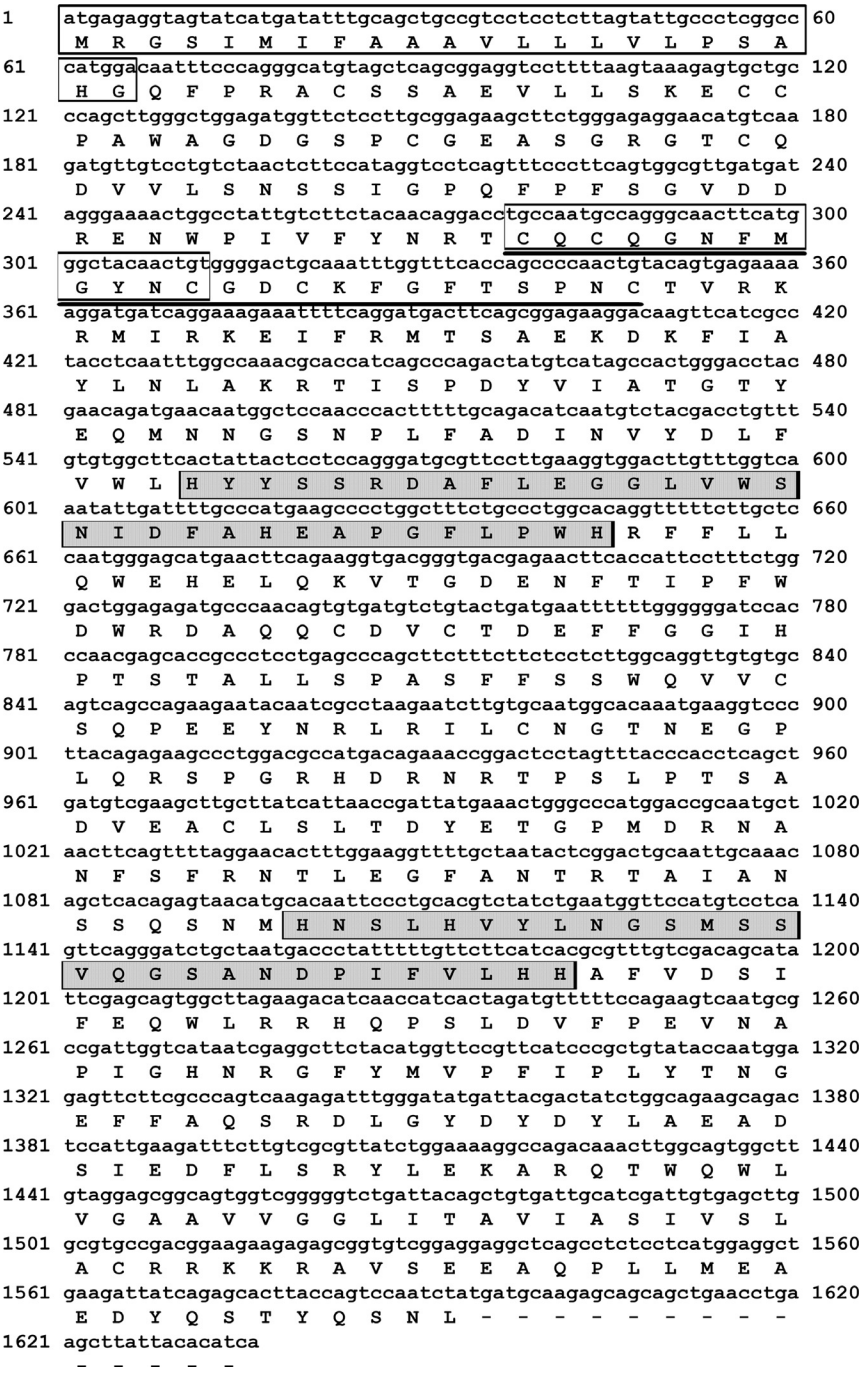

Figure 2 Bufo bufo tyrosinase cDNA and deduced aminoacid sequences (GenBank accession n. FM864217; B6VPX8. (□) signal peptide; (□) EGF-like domain; (——) laminin-type EGF-like domain; CuA and CuB copper binding sites are evidenced by gray bars and dark bars. Putative signal peptide (underlined) was predicted using SignalP 4.1 Server (http://www.cbs.dtu.dk/services/SignalP/), (Nordahl et al., 2011). Searches for EGF-like domain and laminin-type EGF-like domain were conducted at PROSITE (http://prosite.expasy.org/scanprosite/) (De Castro et al., 2006). Functional analysis of protein by classifying them into families and predicting domains and important sites were performed using InterPro (Jones et al., 2014); protein sequence analysis & classification (https://www.ebi.ac.uk/interpro/search/sequence-search) (Jones et al., 2014).

2.10. Data analysis and statistics

Statistical analysis was performed by unpaired Student's *t*-test or One-Way ANOVA test (PAST Paleontological Statistics software Version 3.0) (Hammer et al., 2001). Data analysis was carried out using the ABI 7300 SDS System software version 1.4 (Applied Biosystems). Gene Expression Macro™ Version 1.1. All the biological replicates were used to calculate the average Ct value. Phylogenetic trees were constructed by the maximum likelihood method, using the Molecular Evolution-

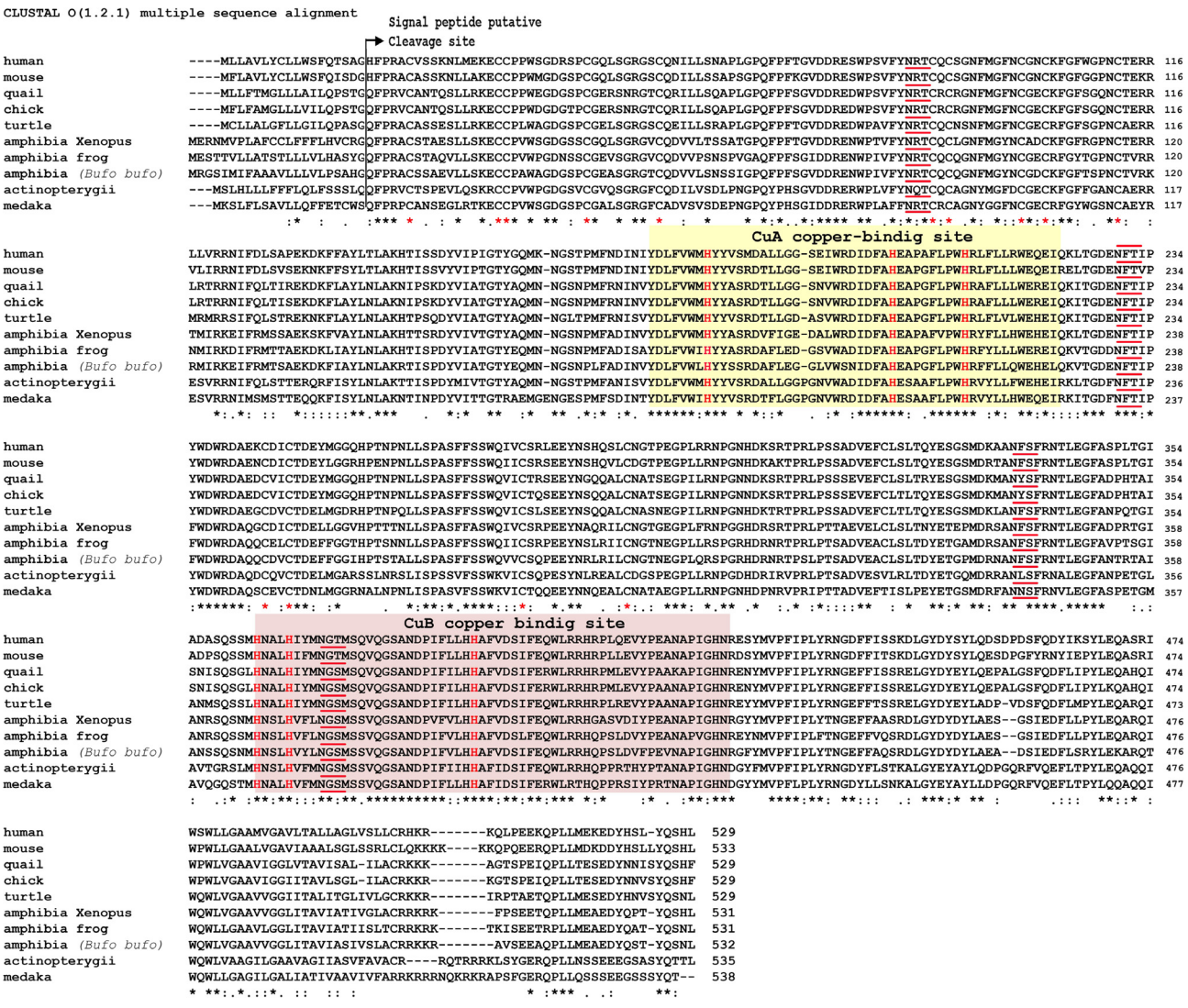

Figure 3 Alignment of deduced amino acid sequences of vertebrate tyrosinases. Deduced amino acid sequences from cDNA clones of *Bufo bufo* B6VPX8 are aligned with previously identified sequences of human (*Homo sapiens* P14679), mouse (*Mus musculus* P11344), quail (*Coturnix coturnix japonica* Q08410), chicken (*Gallus gallus* P55024), turtle (*Pelodiscus sinensis* K7GG37), frog (*Pelophylax nigromaculatus* Q04604), amphibia (*Xenopus tropicalis* F7CL37, *Pelophylax nigromaculatus* Q04604), actinopterygii (*Danio rerio* Q6DGE4) and medaka fish (*Oryzias latipes* P55025) tyrosinases. Tyrosinases sequences were aligned using the CLUSTAL W2 program. The two copper binding sites of tyrosinase (CuA and CuB) are boxed and conserved histidine residues are indicated in red. Conserved cysteine residues in red (*). Putative signal peptide cleavage site ►. Four conserved putative *N*-glycosylation sites are underlined in red. Gaps introduced to maximize sequence homology are represented by dashes. Asterisks indicate identical amino acids.

ary Genetics Analysis (MEGA 7.0) software, (Saitou and Nei, 1987; Kumar et al., 2016).

3. Results

3.1. Nucleotide sequence and primary protein sequence

The nucleotide sequence FM864217 of *B. bufo* tyrosinase cDNA is long 1593 bp and the deduced primary protein sequence B6VPX8, as expected, is long 531 aminoacids as shown in Fig. 2. The gray bars indicate the sequences of tyrosinase cDNA coding for CuA and CuB copper binding sites and the deduced polypeptide primary structures. As presented in Fig. 3 the CuA and CuB copper binding sites of *B. bufo* tyrosinase are highly conserved throughout the phylogenetic scale, from Amphibia to Homo, but in reality from bacteria to man (Prota, 1992). In these regions, which are also found in plant tyrosinases, six conserved histidine residues, that are symmetrically arranged, are believed to form a binuclear copper center and are crucial for the copper-binding and/or enzymatic activity (Hearing and Tsukamoto, 1991; Kanteev et al., 2015). There are 14 cysteine residues at conserved positions distributed unevenly in the sequences as shown in Fig. 3. From Fig. 3 it might erroneously be deduced that, due to the high homology of *B. bufo* tyrosinase active site aminoacid sequence

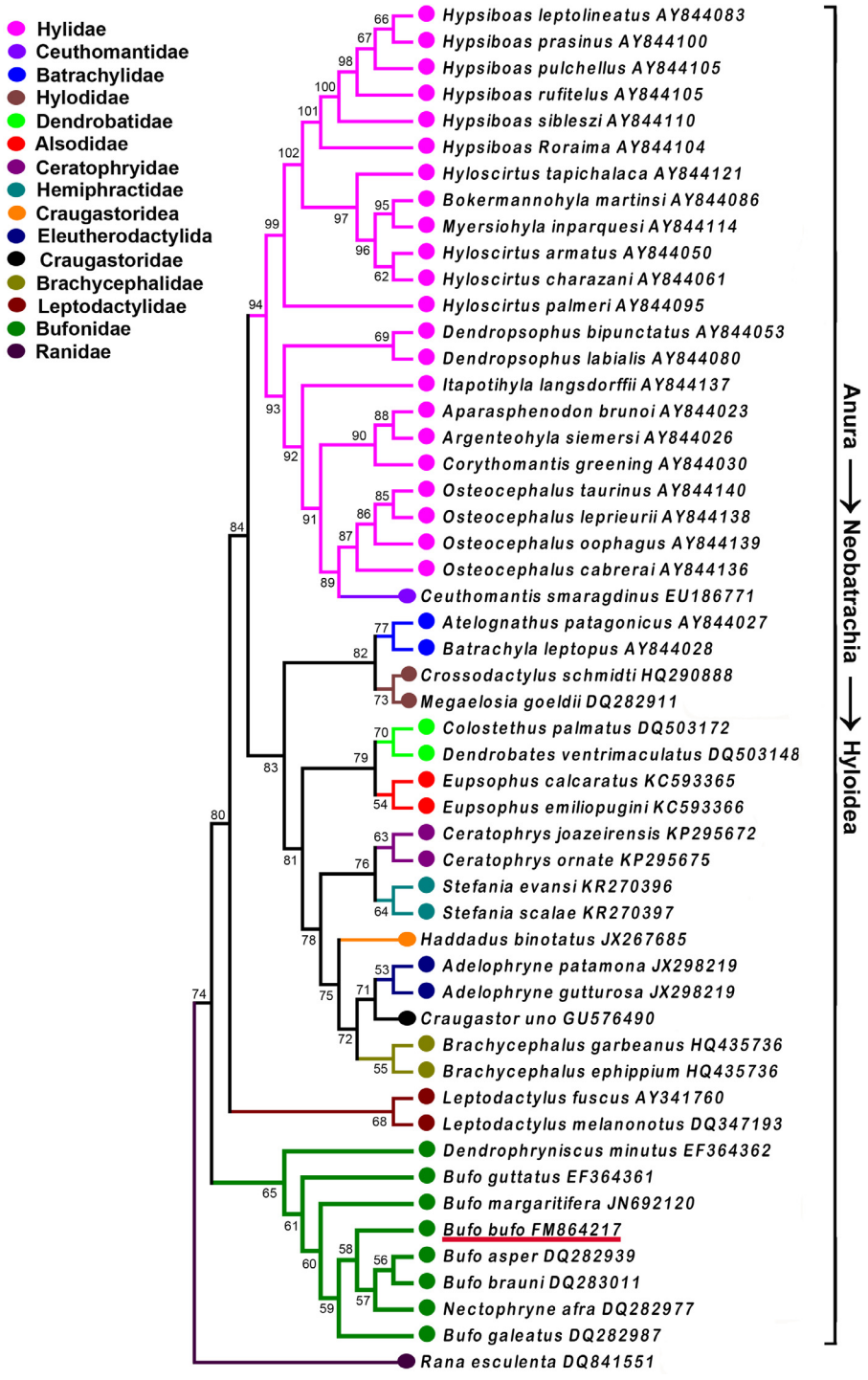

Figure 4 Evolutionary relationships of anura taxa tyrosinase genes. Nucleotide accession numbers for the sequences used to construct this dendrogram are given close to the species name. The evolutionary history was inferred using the Neighbor-Joining method (Saitou and Nei, 1987). The optimal tree with the sum of branch length = 1.49899421 is shown. The evolutionary distances were computed using the Maximum Composite Likelihood method (Tamura et al., 2004) and are in the units of the number of base substitutions per site. The analysis involved 52 nucleotide sequences. All positions containing gaps and missing data were eliminated. There were a total of 313 positions in the final dataset. Evolutionary analyses were conducted in MEGA7 (Kumar et al., 2016).

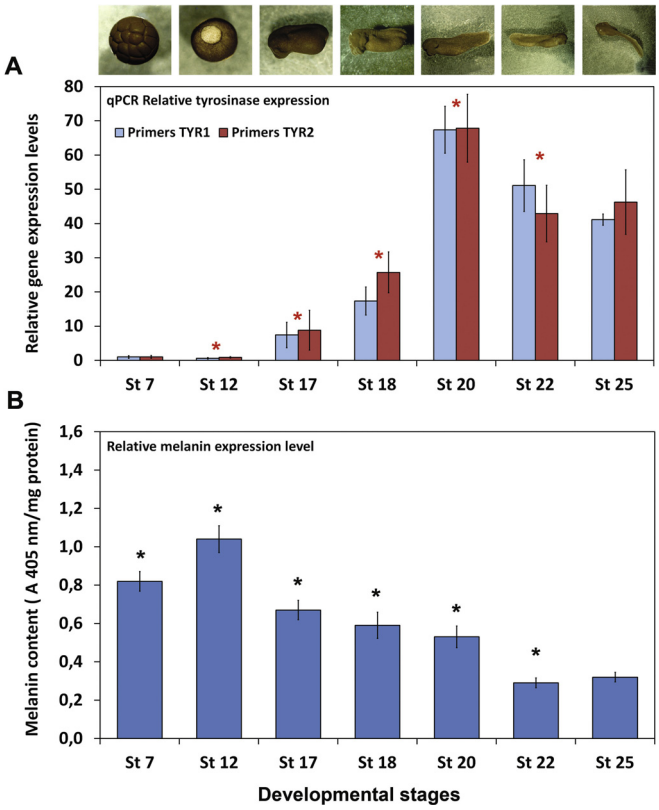

Figure 5 qRT-PCR expression level of tyrosinase gene and melanin pigment content at the different developmental stages of *Bufo bufo*. (A) Expression levels of TYR mRNA at different developmental stages of *Bufo bufo* measured by qRT-PCR. (B) About 50 embryos at the different developmental stage were dissolved in lysis buffer; the melanin pigment content was spectrophotometrically determined at 405 nm and the obtained values were normalized to the total protein concentration. Data represent mean ± SEM of triplicate assays. *Significant differences ($P < 0.05$) are indicated by asterisks.

to those of *Pelophylax nigromaculatus* and *Xenopus tropicalis* the tyrosinases of these species are closely related to the *B. bufo* one (Zheng et al., 2010). On the contrary, no close relationship is found when comparing the base sequence coding for *B. bufo* tyrosinase to those of *Pelophylax nigromaculatus* and other different anurans as shown in Fig. 4: the closest tyrosinase coding sequences are those of Bufonidae, as expected. The phylogenetic tree shown is in congruence with previously published phylogenetic trees (Ruvinsky and Maxson, 1996; Salducci et al., 2005).

3.2. Tyrosinase levels in the developmental stages of Bufo bufo

B. bufo developmental stages 7, 12, 17, 18, 20, 22 and 25 were investigated for tyrosinase mRNA levels by RT-PCR and qRT-PCR.

Two different couples of specific primers, prepared from the *B. bufo* tyrosinase cDNA sequence were used to amplify by qRT-PCR tyrosinase cDNA and thus to detect the *B. bufo* developmental stage at which the gene is expressed. As shown in Fig. 5A, during *B. bufo* development tyrosinase mRNA is expressed at the developmental stage 17–18 and the maximal expression occurs at stage 20 in accord with tyrosinase activity (L-DOPA oxidase), that significantly increases from stage 18 to stage 25 as shown in Fig. 6A and B. As expected tyrosinase gene and activity expression curves are parallel to the oxygen consumption of *B. bufo* embryo, when an increase of tyrosinase gene and activity expression and oxygen consumption occur, i.e. after the developmental stages 17–19 when blood circulation starts as shown in Fig. 6B and C. As mitochondrial respiratory chain generates reactive oxygen species (ROS), as well as melanogenesis, it is interesting that the tyrosinase promoter of the anuran *Rana nigromaculata* has two ROS responsive elements (GenBank: D37779.1). As shown in Fig. 7, the expression analysis conducted with the RT-PCR technique essentially confirms the data of the qRT-PCR by the intensity of the electrophoretic band of 1510 bp of the tyrosinase sequence. The levels of melanin seem initially to decrease and then to stabilize in the course of development as shown in Fig. 4B. During *Rana pipiens* development tyrosinase mRNA is accumulated at stage 13 (neural plate) (Gaulton and Triplett, 1983).

4. Discussion

The tyrosinase mRNA expression profile during *B. bufo* development is in full agreement with the enzymatic activity expression as detected by biochemical methods (Miranda et al., 1982).

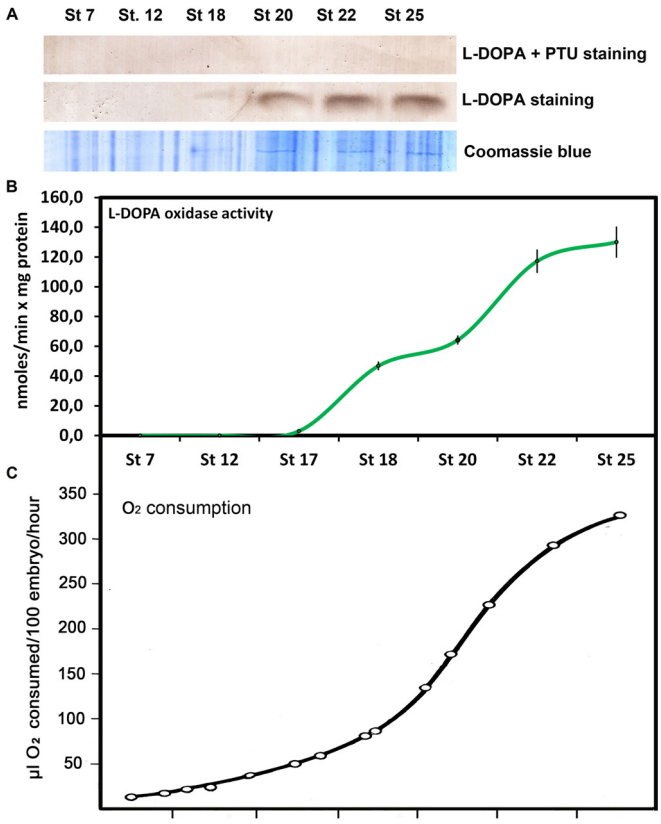

Figure 6 Tyrosinase activity. (A) Native SDS electrophoretic evidence of the catecholase activity at different *Bufo bufo* developmental stages. 15 µg protein of melanosome extract was loaded onto polyacrylamide gel and the gels were stained with L-DOPA + PTU, L-DOPA and Coomassie brilliant G250 blue. (B) The tyrosinase activity was measured spectrophotometrically, by using as substrate 5 mM L-DOPA dissolved in 100 mM sodium phosphate buffer pH 6.8, at 25 °C (by recording dopachrome production at 475 nm). (C) Curve of O_2 consumption during *Bufo bufo* development (Petrucci, 1961). Data represent mean ± SEM of triplicate assays.

The expression of tyrosinase mRNA at the developmental stages 17–18 is clearly evident as well the L-DOPA oxidase activity of tyrosinase as shown in Fig. 5A and B, while neither enzyme activity nor mRNA expression were found before those developmental stages, contrary to *R. pipiens* development (Gaulton and Triplett, 1983). According to our findings during *B. bufo* development, L-DOPA oxidase activity at very low levels appears at stage 17 (tail bud stage) and at stage 18 (muscular response) both tyrosinase L-DOPA oxidase activity and mRNA expressions occur overtly. These findings while confirming the expression of tyrosinase gene after late gastrula (developmental stage 12) show a difference between *B. bufo* and *R. pipiens* developments, as in *R. pipiens* tyrosinase mRNA was found starting from the neural plate stage, by hybridization of tyrosinase cDNA to total embryo RNA and L-DOPA oxidase activity at developmental stage 20 (hatching) (Gaulton and Triplett, 1983). The different stages of tyrosinase mRNA (17–18) and L-DOPA oxidase activity (17–18) expressions during *B. bufo* development, compared to *R. pipiens*, respectively at stages 13 and 20 may be ascribed to the different techniques used to detect mRNA expression, PCR versus cDNA/RNA hybridization, and L-DOPA oxidase activity assay of the enzyme extracted from melanosomes versus ammonium sulfate protein fractions of total embryo homogenates. However, the different developmental conditions of *B. bufo* and *R. pipiens*, such as environmental temperature and exposition to solar radiation that may affect melanin pigmentation (Bagnara, 1985) should also be taken into account.

5. Conclusion

As a final conclusion we have here demonstrated that *B. bufo* embryo melanin is of maternal origin, at least until developmental stage 17, when first a detectable L-DOPA oxidase activity and embryo tyrosinase gene transcription are evident. This work shows that during *B. bufo* development tyrosinase gene and activity expressions occur starting from the developmental stage 17; differently in *R. pipiens* the tyrosinase gene expression occurs at the developmental stage 13 and the enzymatic activity at stage 20. As tyrosinase is an oxidase, we have investigated if the curves of enzymatic activity and O_2 consumption during *B. bufo* development are correlated. The tyrosinase expression curve is parallel to that of O_2 consumption. As previous authors report (Boell et al., 1971) in all amphibian species tested the increase of cytochrome c oxidase and then of oxygen consumption occurs at the stage when motility begins (stage 18 muscular response). As tyrosinase in an oxidase, it appears logical that when embryo respiration increases, due to O_2 transport in the embryo tissues, also the oxidation of

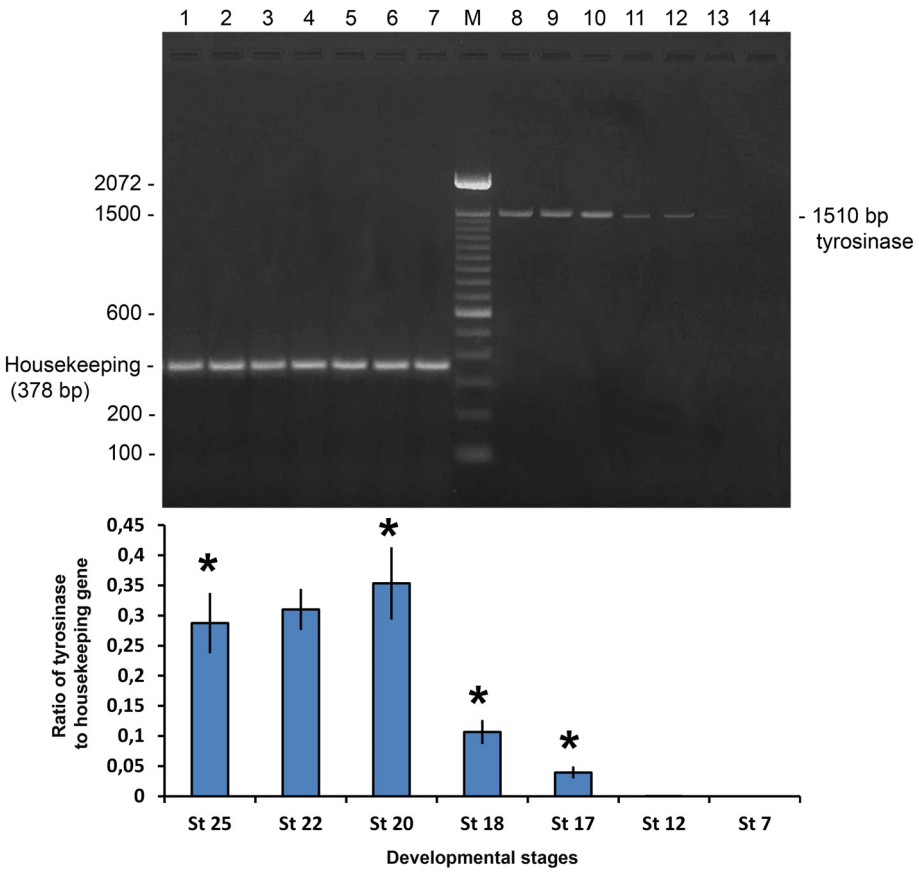

Figure 7 Quantification of *Bufo bufo* tyrosinase mRNA by RT-PCR and 1.5% agarose gel electrophoresis. Tyrosinase mRNA expression was determined by RT-PCR of total mRNA obtained from different developmental stages of *Bufo bufo*. NADH dehydrogenase subunit I expression (378 bp) was used as an internal housekeeping mRNA. M: markers (Invitrogen's 100 bp DNA Ladder); lane 1–8 stage 25; lane 2–9 stage 22; lane 3–10 stage 20; lane 4–11 stages 18; lane 5–12 stage 17; lane 6–13 stage 12; lane 7–14 stage 7. Quantification of tyrosinase and NADH dehydrogenase subunit I was accomplished densitometrically measuring the ethidium bromide binding intensity of the UV-irradiated PCR products by a Nanodrop 2000 spectrophotometer (Thermo Scientific, Waltham, WA). The housekeeping gene NADH dehydrogenase subunit I was used for normalization. Data represent mean ± SEM (n 3). *Significant differences ($P < 0.05$) are indicated.

tyrosinase substrates should increase and contribute to the embryo O_2 consumption increase.

Appendix A. Supplementary data

Supplementary data associated with this article can be found, in the online version, at http://dx.doi.org/10.1016/j.sjbs.2016.10.018.

References

Andersen, C.L., Jensen, J.L., Ørntoft, T.F., 2004. Normalization of real-time quantitative reverse transcription-PCR data: a model-based variance estimation approach to identify genes suited for normalization, applied to bladder and colon cancer data sets. Cancer Res. 64 (15), 5245–5250.

Bagnara, J.T., 1985. The amphibian egg as a pigment cell. Pigment Cell Res. 6, 277–281.

Benson, S.C., Triplett, E.L., 1974. The synthesis and activity of tyrosinase during development of the frog *Rana pipiens*. Dev. Biol. 40 (2), 270–282.

Boell, E.J., D'Anna, T., Greenfield, P., Petrucci, D., 1971. Cytochrome oxidase activity during amphibian development. J. Exp. Zool. 178 (2), 151–163.

De Castro, E., Sigrist, C.J.A., Gattiker, A., Bulliard, V., Langendijk-Genevaux, P.S., Gasteiger, E., Bairoch, A., Hulo, N., 2006. ScanProsite: detection of PROSITE signature matches and ProRule-associated functional and structural residues in proteins. Nucleic Acids Res. 34. Web Server issue: W362–W365.

Eppig, J.J., Dumont, J.N., 1974. Oogenesis in *Xenopus laevis* (Daudin): II. The induction and sub-cellular localization of tyrosinase activity in developing oocytes. Dev. Biol. 36 (2), 330–342.

Gaulton, G.N., Triplett, E.L., 1983a. Control of tyrosinase gene expression and its relationship to neural crest induction in *Rana pipiens*. I. Isolation and characterization of amphibian tyrosinase mRNA. J. Biol. Chem. 258 (24), 14839–14844.

Gaulton, G.N., Triplett, E.L., 1983b. Control of tyrosinase gene expression and its relationship to neural crest induction in *Rana pipiens*. II. Measurement of tyrosinase mRNA accumulation during early embryogenesis using a specific cDNA probe. J. Biol. Chem. 258 (24), 14845–14849.

Hammer, Ø., Harper, D.A.T., Ryan, P.D., 2001. PAST: paleontological statistics software package for education and data analysis. Palaeontol. Electron. 4 (1), 9–18.

Hastings, D., Burggren, W., 1995. Developmental changes in oxygen consumption regulation in larvae of the South African clawed frog *Xenopus laevis*. J. Exp. Biol. 198 (Pt12), 2465–2475.

Hearing, V.J., Tsukamoto, K., 1991. Enzymatic control of pigmentation in mammals. FASEB J. 5 (14), 2902–2909.

Jones, P., Binns, D., Chang, H., Fraser, M., Li, W., McAnulla, C., McWilliam, H., Maslen, J., Mitchell, A., Nuka, R., Pesseat, S., Quinn, A.F., Sangrador-Vegas, A., Scheremetjew, M., Yong, S., Lopez, R., Hunter, S., 2014. InterProScan 5: genome-scale protein function classification. Bioinformatics 29, 1–5.

Kanteev, M., Goldfeder, M., Fishman, A., 2015. Structure–function correlations in tyrosinases. Protein Sci. 24 (9), 1360–1369.

Kumar, S., Stecher, G., Tamura, K., 2016. MEGA7: molecular evolutionary genetics analysis version 7.0 for bigger datasets. Mol. Biol. Evol. 33, 1870–1874.

Laemmli, U.K., 1970. Cleavage of structural proteins during the assembly of the head of bacteriophage T4. Nature 277 (5259), 680–685.

Mason, H.S., 1948. The chemistry of melanin. III. Mechanism of the oxidation of dihydroxyphenylalanine by tyrosinase. J. Biol. Chem. 172 (1), 83–99.

Mason, H.S., 1965. Oxidases. Annu. Rev. Biochem. 34, 594–634.

Miranda, M., Botti, D., Ragnelli, A.M., Di Cola, M., 1982. A study on melanogenesis and catecholamine biosynthesis during *Bufo bufo* development. J. Exp. Zool. 224 (2), 217–222.

Nicolaus, R.A., 1968. Melanins. Hermann (Ed.), Paris.

Nordahl, T., Søren Brunak, P., von Heijne, G., Nielsen, H., 2011. SignalP 4.0: discriminating signal peptides from transmembrane regions. Nat. Methods 8, 785–786.

Petrucci, D., 1961. The RQ and the incorporation of C-14-O_2 in the course of the embryonal development of *Bufo bufo*. Riv. Biol. 54, 339–354.

Pfaffl, M.W., Tichopad, A., Prgomet, C., Neuvians, T.P., 2004. Determination of stable housekeeping genes, differentially regulated target genes and sample integrity: BestKeeper—excel-based tool using pair-wise correlations. Biotechnol. Lett. 26 (6), 509–515.

Prota, G., 1992. Melanins and Melanogenesis. Academic Press Inc, San Diego, California.

Robb, D.A. (Ed.), 1984. TyrosinaseLontie, R (Ed.). Copper Proteins and Copper Enzymes, vol. II. CRC Press, Boca Raton.

Ruvinsky, I., Maxson, L.R., 1996. Phylogenetic relationships among bufonoid frogs (Anura: Neobatrachia) inferred from mitochondrial DNA sequences. Mol. Phylogenet. Evol. 5, 533–547.

Saitou, N., Nei, M., 1987. The neighbor-joining method: a new method for reconstructing phylogenetic trees. Mol. Biol. Evol. 4, 406–425.

Salducci, M.D., Marty, C., Fouquet, A., Gilles, A., 2005. Phylogenetic relationships and biodiversity in hylids (Anura: Hylidae) from French guiana. C R Biol. 328 (10–11), 1009–1024.

Sanchez-Ferrer, A., Rodriguez-Lopez, J.N., Garcia-Canovas, F., Garcia-Carmona, F., 1995. Tyrosinase: a comprehensive review of its mechanism. Biochim. Biophys. Acta 1247 (1), 1–11.

Seyeon, P., Hana, C., Yun Joo, K., 2013. Inhibition of isorhamnetin on β-catenin/Tcf signaling and β-catenin-activated melanogenesis. J. Basic Appl. Sci. 9, 401–409.

Shumway, W., 1940. Stages in the normal development of *Rana pipiens*. Anat. Rec. 78 (2), 139–147.

Silver, N., Best, S., Jiang, J., Thein, S.L., 2006. Selection of housekeeping genes for gene expression studies in human reticulocytes using real-time PCR. BMC Mol. Biol. 7 (1), 33.

Solano, F., 2014. Melanins: skin pigments and much more-types, structural models, biological functions, and formation routes. New J. Sci. 2014, 1–28.

Tamura, K., Nei, M., Kumar, S., 2004. Prospects for inferring very large phylogenies by using the Neighbor-Joining method. Proc. Natl. Acad. Sci. U.S.A. 101, 11030–11035.

Taylor, J.D., Hadley, M.E., 1972. The fate of amphibian egg melanosomes. J. Cell Biol. 52, 493–501.

Vandesompele, J., De Preter, K., Pattyn, F., Poppe, B., Van Roy, N., De Paepe, A., Speleman, F., 2002. Accurate normalization of real-time quantitative RT-PCR data by geometric averaging of multiple internal control genes. Genome Biol. 3 (7). RESEARCH0034.

Zheng, H., Li, X., Zhou, R., Li, L., Guo, X., Kang, J., Li, D., 2010. Bioinformatics analysis of Tyrosinase-Related Protein 1 gene (*TYRP1*) from different species. Front. Agr. China 4 (1), 109–115.